Gamma Interferon Regulates Contraction of the Influenza Virus-Specific CD8 T Cell Response and Limits the Size of the Memory Population

Nayana Prabhu,[a,b] Adrian W. Ho,[a] Kenneth H. S. Wong,[a] Paul Edward Hutchinson,[a] Yen Leong Chua,[a] Matheswaran Kandasamy,[c] Debbie C. P. Lee,[a] Baalasubramanian Sivasankar,[c] David Michael Kemeny[a,b]

Immunology Programme and Department of Microbiology, National University of Singapore, Singapore[a]; NUS Graduate School for Integrated Sciences and Engineering, National University of Singapore, Singapore[b]; Infection & Immunity Programme, Singapore Institute for Clinical Sciences, Agency for Science, Technology and Research (A*STAR), Singapore[c]

The factors that regulate the contraction of the CD8 T cell response and the magnitude of the memory cell population against localized mucosal infections such as influenza are important for generation of efficient vaccines but are currently undefined. In this study, we used a mouse model of influenza to demonstrate that the absence of gamma interferon (IFN-γ) or IFN-γ receptor 1 (IFN-γR1) leads to aberrant contraction of antigen-specific CD8 T cell responses. The increased accumulation of the effector CD8 T cell population was independent of viral load. Reduced contraction was associated with an increased fraction of CD8 T cells expressing the interleukin-7 receptor (IL-7R) at the peak of the response, resulting in enhanced numbers of memory/memory precursor cells in IFN-γ$^{-/-}$ and IFN-γR$^{-/-}$ compared to wild-type (WT) mice. Blockade of IL-7 within the lungs of IFN-γ$^{-/-}$ mice restored the contraction of influenza virus-specific CD8 T cells, indicating that IL-7R is important for survival and is not simply a consequence of the lack of IFN-γ signaling. Finally, enhanced CD8 T cell recall responses and accelerated viral clearance were observed in the IFN-γ$^{-/-}$ and IFN-γR$^{-/-}$ mice after rechallenge with a heterologous strain of influenza virus, confirming that higher frequencies of memory precursors are formed in the absence of IFN-γ signaling. In summary, we have identified IFN-γ as an important regulator of localized viral immunity that promotes the contraction of antigen-specific CD8 T cells and inhibits memory precursor formation, thereby limiting the size of the memory cell population after an influenza virus infection.

Annual influenza epidemics cause up to 500,000 deaths annually and impose a serious economic burden in the form of health care and hospitalization costs all around the world. Efforts are continuously being made to generate better vaccines against influenza. Vaccines targeting antibody responses against the surface proteins are protective only against the same or similar strains of virus due to the constant antigenic drift and shift in the surface hemagglutinin and neuraminidase proteins of the virus (1). Since CD8 T cells are generally formed against the conserved internal proteins of the virus (2, 3), newer generations of vaccines aim to generate better CD8 T cell memory responses against influenza. However, the factors which control memory CD8 T cell generation in response to influenza virus are not yet clearly understood.

CD8 T cells contribute to immunity against viral infections such as influenza by promoting viral clearance and hence host recovery (4–6). During an influenza virus infection, the virus-specific CD8 T cell response is initiated in the lung draining lymph node (7), and the activated cells infiltrate the lung, where they exhibit effector function (8, 9). The CD8 T cells are exposed to a highly inflammatory environment in the lung. This cytokine milieu programs the CD8 T cells to undergo additional proliferation, to acquire effector function (8, 10), and to undergo programmed cell death or differentiate into memory cells after viral clearance (11–13). The signals that determine CD8 T cell fate in an influenza virus infection are not fully understood. Several cytokines, such as interleukin-2 (IL-2), IL-7, and IL-15, play a homeostatic role in T cell memory. IL-2 induces the transcriptional programs that support generation of terminal effector CD8 T cells as opposed to

memory cells (14, 15). IL-7 and IL-15 support the formation of long-lived memory T cells (16, 17).

Previous studies on the role of gamma interferon (IFN-γ) in the contraction of the CD8 T cell response have focused on systemic infections with organisms such as lymphocytic choriomeningitis virus (LCMV), cytomegalovirus (CMV), vesicular stomatitis virus (VSV), and *Listeria monocytogenes* (11, 18–21). Thus far, no data have described a role for IFN-γ in CD8 T cell contraction after an acute localized infection. Although IFN-γ was found to play a critical role in the contraction of CD8 T cells following LCMV and *L. monocytogenes* infections (11, 18, 19), this process was reported to be independent of IFN-γ in VSV and CMV infections (20, 21). Therefore, to investigate whether IFN-γ is involved in mediating CD8 T cell contraction during a localized infection, we utilized influenza virus, whose replication is confined within the lung and which does not disseminate to other organs.

In this study, we demonstrate that IFN-γ plays a key role in regulating the survival of influenza virus-specific CD8 T cells. We show that IFN-γ negatively regulates expression of the IL-7 recep-

tor (IL-7R) on the surface of antigen-specific CD8 T cells and hence limits their ability to respond to IL-7. This encourages their death during the contraction phase, thereby limiting the number of memory cell precursors formed after an influenza virus infection. We also show that the increased memory precursor frequency in the absence of IFN-γ signaling correlates with an increased CD8 T cell response, and hence better viral clearance during a secondary influenza virus challenge. Thus, our study shows for the first time that IFN-γ not only regulates the contraction phase but also controls the generation of the antigen-specific memory CD8 T cell response to a localized mucosal infection such as influenza.

MATERIALS AND METHODS

Mice. C57BL/6 mice (8 to 10 weeks old) were purchased from the National University of Singapore breeding center (CARE). IFN-$\gamma^{-/-}$ and IFN-$\gamma R^{-/-}$ mice were purchased from the Jackson Laboratory (Bar Harbor, ME). OT-1 mice were purchased from Charles River Laboratories. The OT-1 mice were crossbred with the IFN-$\gamma^{-/-}$ mice for 3 to 5 generations to generate OT-1x IFN-$\gamma^{-/-}$ mice. Mice were matched by age and sex for each experiment. All mice were maintained under pathogen-free conditions in a satellite animal housing unit and were transferred to an animal biosafety level 2 (ABSL2) facility for experiments involving infection with influenza virus. All experiments were performed in strict accordance with the guidelines of the National Advisory Committee for Laboratory Animal Research (NACLAR), Singapore, and the Institutional Animal Care and Use Committee (IACUC) of the National University of Singapore approved the protocols (protocol numbers 137/08 and 087/10).

Viruses and determination of viral titers. Influenza virus strain A/PR/8/34 (VR-95) was purchased from the American Type Culture Collection. Recombinant influenza A/PR/8/34 virus containing the chicken OVA epitope SIINFEKL (PR/8-OT-1) was a gift from Paul Thomas (St. Jude Children's Research Hospital, Memphis, TN). Influenza viruses A/PR/8/34 (H1N1), A/HKx31 (H3N2), and PR/8-OT-1 (with the SIINFEKL epitope) were grown in 10-day-old embryonated chicken eggs as previously described (7). Viral titers in the lungs were determined as described previously (7). Briefly, serial 10-fold dilutions of lung homogenates were allowed to adsorb onto confluent monolayers of Madin-Darby canine kidney (MDCK) cells (ATCC CCL-34) on a 24-well plate for 1 h. The supernatant was then removed and replaced with 1% agarose supplemented with serum-free Dulbecco's modified Eagle medium (DMEM) (Invitrogen, Life Technologies, Singapore) and 2 μg/ml tosylsulfonyl phenylalanyl chloromethyl ketone (TPCK)-treated trypsin (Pierce, Research Instruments, Singapore). Plates were incubated for 3 days at 37°C in 5% CO_2. Agarose overlays were then removed, and the plaques were visualized and enumerated after addition of crystal violet stain.

Infection of mice. Mice were anesthetized by intraperitoneal (i.p.) injections of ketamine at 100 mg/kg of body weight (Parnell Laboratories, Australia) and medetomidine at 15 mg/kg (Pfizer, New Zealand). Intranasal inoculations were carried out with the required dose of the virus in 20 μl phosphate-buffered saline (PBS), after which 5 mg/kg of atipamezole (Pfizer, Australia) was administered by i.p. injection to reverse the effects of the anesthetic. The mice were then monitored daily for weight loss and mortality for 14 days after the infection. Mice that lost more than 25% of their original body weight were euthanized.

Determination of levels of viral RNA in the lungs. Quantitative reverse transcription-PCR (qRT-PCR) on viral mRNA was performed as described earlier (22). Briefly, total RNA was obtained from the lung tissue by use of an RNeasy kit (Qiagen) according to the manufacturer's protocol, after which the cDNA was synthesized using a random hexamer. Real-time PCR was performed on an ABI7500 real-time PCR system using SYBR green (Applied Biosystems). Primers used for qRT-PCR were as

follows: Influenza M-protein forward, 5′-GGACTGCAGCGTTAGACGC TT-3′; Influenza M-protein reverse, 5′-CATCCTGTTGTATATGAGGC CCAT-3′; beta-actin forward, 5′-AGAGGGAAATCGTGCGTGAC-3′; and beta-actin reverse, 5′-CAATAGTGATGACCTGGCCGT-3′.

Flow cytometry. Anti-CD3 (clone 17A2), anti-CD11b (clone M1/70), anti-B220 (clone RA3-6B2), anti-CD127 (clone A7R34), anti-CD215 (clone DNT15Ra), and anti-CD107a (clone eBio1D4B) antibodies were purchased from eBioscience, Immunocell, Singapore. Anti-CD8α (clone 53-6.7), anti-CD11c (clone N418), anti-CD25 (clone PC61), anti-CD122 (clone TM-β1), and anti-CD132 (clone TUGm2) were purchased from Biolegend, Singapore. Anti-Gr-1 (clone RB6-8C5) was purchased from BD Biosciences, Singapore. An R-phycoerythrin (R-PE)-labeled Pro5 major histocompatibility complex (MHC) pentamer for H-2D^b/ASNEN-METM binding to NP$_{366}$ was purchased from ProImmune Ltd., United Kingdom, and staining of virus-specific CD8$^+$ T cells was performed according to the manufacturer's protocol. Neutralizing polyclonal antibody against IL-7 was obtained from R&D Systems, Singapore. 7-Aminoactinomycin D (7-AAD) was purchased from Sigma-Aldrich, Singapore. Acquisition of samples was performed on a Cyan ADP (Beckman Coulter, CA) or Fortessa (BD, NJ) instrument. Data were analyzed by FlowJo software (Treestar). Cells were sorted using a MoFlo cell sorting system (Beckman Coulter, Singapore).

Isolation of CD8 T cells from BAL fluid and lungs. Mice were sacrificed using carbon dioxide asphyxiation. Bronchoalveolar lavage (BAL) fluid samples were collected by three 0.7-ml instillations of PBS into the tracheas of cannulated mice. Red blood cells (RBCs) were lysed using RBC lysis buffer, and after centrifugation, the cell pellet was stained with the appropriate antibodies. Cells were isolated from the lungs of infected mice as described previously (23), with a few modifications. Briefly, lungs were excised, chopped into small pieces, and digested in 0.5 mg/ml Liberase CI (Roche Diagnostics, Singapore) for 45 min at 37°C before physical disruption into single-cell suspensions by passage through a 61-μm cell strainer (Fischer Scientific, Singapore). Single-cell suspensions were then layered on Ficoll-Paque (GE Healthcare, Scimed, Singapore) and centrifuged at 600 × g for 20 min at room temperature. Cells accumulating at the interface were collected, washed twice, and stained with antibodies as required.

Isolation of CD8 T cells from spleens and lymph nodes. Spleens and lymph nodes were collected from euthanized mice. Single-cell suspensions were layered on Ficoll-Paque (GE Healthcare, Singapore) and centrifuged at 600 × g for 20 min at room temperature. Cells accumulating at the interface were collected, washed twice, incubated with anti-CD8a-conjugated magnetically activated cell sorting (MACS) beads (Miltenyi Biotec, Germany), and then isolated by passing the cells through a MACS column.

^{51}Cr release assay for cytotoxicity. EL4 target cells were labeled with radioactive ^{51}Cr (PerkinElmer, Singapore) and pulsed with 10 mg/ml of ASNENMETM peptide (Mimotopes, Australia). Purified CD8 cells from the lungs were cultured with target cells at the desired ratios for 6 h before supernatants were harvested. Supernatants were loaded into a 96-well Luma plate and left to dry overnight. Radioactive counts were determined using Beckman Top Count (PerkinElmer, Singapore).

Statistical analysis. Statistical analysis was performed using GraphPad Prism. Comparisons across groups were made using one-way analysis of variance (ANOVA), and paired comparisons were performed using Student's t test or the Mann-Whitney test, as appropriate. Data are expressed as means ± standard errors of the means (SEM) (P values of <0.05, <0.01, and <0.001 are indicated). Flow cytometric profiles and histograms are representative of repeated experiments.

RESULTS

Increased accumulation of antigen-specific CD8 T cells in IFN-$\gamma^{-/-}$ and IFN-$\gamma R^{-/-}$ mice after influenza virus infection. Inflammatory cues such as IFN-γ are known to play a critical role in the modulation of CD8 T cell responses against LCMV and *Listeria* infections (24). In view of the fact that high levels of IFN-γ are
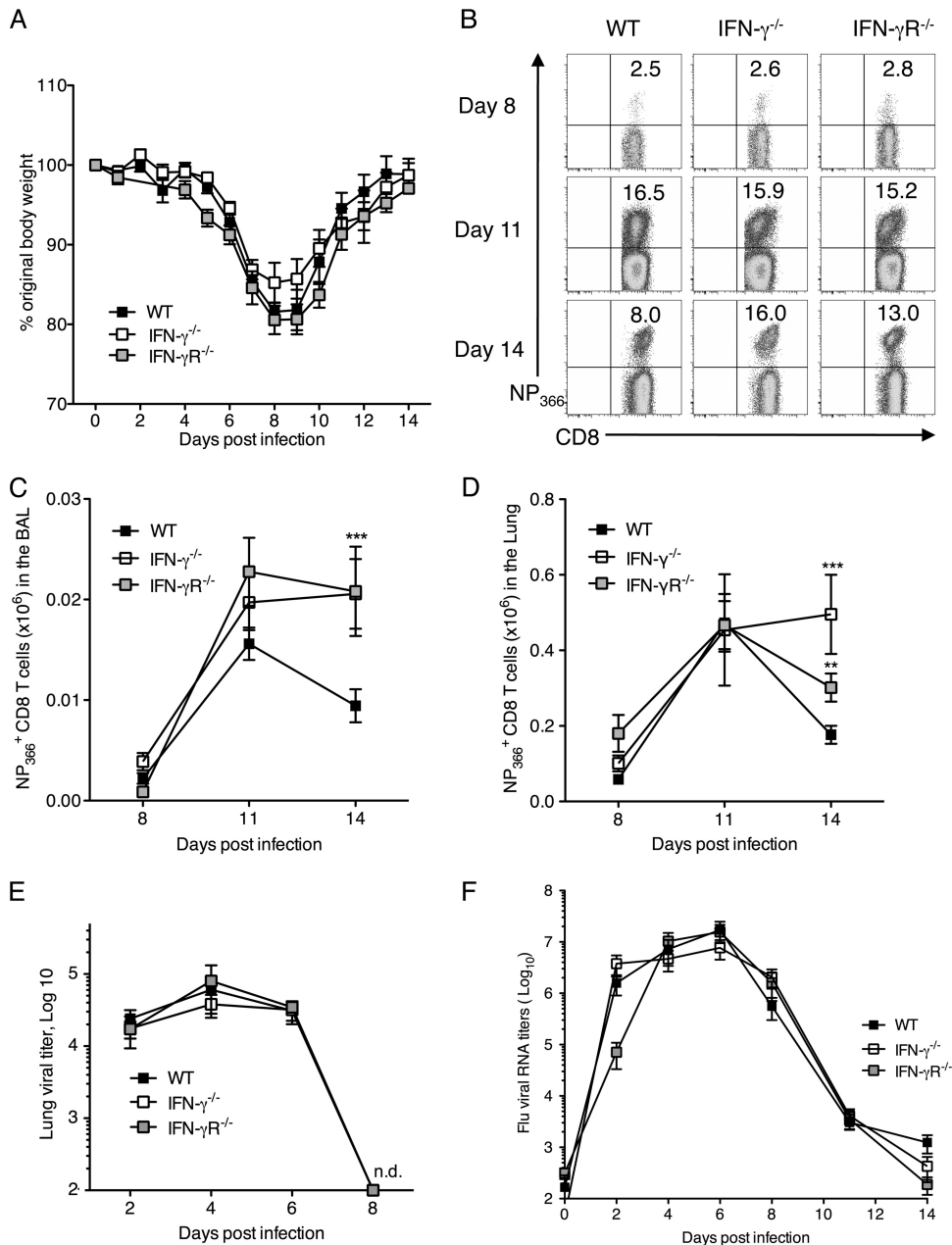
FIG 1 Increased accumulation of antigen-specific CD8 T cells in IFN-$\gamma^{-/-}$ and IFN-γR$^{-/-}$ mice after influenza virus infection. C57BL/6 WT, IFN-$\gamma^{-/-}$, and IFN-γR$^{-/-}$ mice were infected with 5 PFU of influenza A/PR/8/34 virus. (A) Graph showing weight loss in mice over the course of 14 days after infection. Lungs were harvested, and cells were stained with anti-CD3 and anti-CD8 antibodies and the H2-D^b NP$_{366}$ pentamer on the indicated days. (B) Representative flow cytometry plots of the proportion of CD8$^+$ T cells specific for NP$_{366}$ (ASNENMETM) in the lung tissue of WT, IFN-$\gamma^{-/-}$, and IFN-γR$^{-/-}$ mice. Cells were gated on CD3$^+$ CD8$^+$ T cells. Numbers represent percentages of CD8$^+$ T cells in the lung which are NP$_{366}$$^+$. (C and D) Total NP$_{366}$$^+$ CD8 T cell numbers in the BAL fluid (C) and lung tissue (D) across a time course following influenza virus infection of WT, IFN-$\gamma^{-/-}$, and IFN-γR$^{-/-}$ mice. The numbers of CD8$^+$ NP$_{366}$$^+$ cells (means ± SEM) shown were calculated from the total counts and the percentages of cells staining positive. (E) Kinetics of viral loads in the lung tissue of infected mice over a period after infection. (F) Graph showing relative RNA levels of influenza virus M protein in the lungs of infected mice. Data represent means ± SEM. Data were pooled from three independent experiments with 4 or 5 mice/group/experiment. **, $P < 0.01$; ***, $P < 0.001$ (determined using the Mann-Whitney test). n.d., not detected.

found in the lungs during an influenza virus infection (data not shown), we hypothesized that IFN-γ may play an important part in regulating the immune response to influenza virus. We analyzed murine CD8 T cell responses to influenza virus in the presence and absence of IFN-γ signaling. Wild-type (WT), IFN-$\gamma^{-/-}$, and IFN-γR$^{-/-}$ mice were infected with a sublethal dose (5 PFU)

of the A/PR/8/H1N1 strain of influenza virus. The absence of IFN-γ or IFN-γR did not compromise survival, as all infected mice survived the ensuing infection, losing about 20% of their original body weight by day 8 and then regaining their original weight by day 14 postinfection (p.i.) (Fig. 1A). Antigen-specific CD8 T cell responses to influenza virus were measured by enu-

merating the number of cells binding to the dominant epitope in an MHC I pentamer-$D^b NP_{366}$ (ASNENMETM) in the BAL fluid and lung tissue of mice at different time points after infection (Fig. 1B). In WT mice, the proportion and number of NP_{366}^+ CD8 T cells in the BAL fluid (Fig. 1C) and the lung tissue (Fig. 1D) increased substantially after day 8, peaked at day 11, and then decreased. In the IFN-γ$^{-/-}$ and IFN-γR$^{-/-}$ mice, the kinetics of the antigen-specific CD8 T cell response was similar to that in WT mice at the beginning. However, there were significantly larger numbers of NP_{366}^+ CD8 T cells in both the BAL fluid (Fig. 1C) and lung tissue (Fig. 1D) of the IFN-γ$^{-/-}$ and IFN-γR$^{-/-}$ mice than in those of the WT mice on day 14 p.i. By this time, the decline in the numbers of NP_{366}^+ CD8 T cells was clearly evident in the WT mice, while IFN-γ$^{-/-}$ and IFN-γR$^{-/-}$ mice showed no significant decrease in NP_{366}^+ CD8 T cell numbers. We concluded that IFN-γ was not critical for the initiation of the influenza virus-specific CD8 T cell response but may play a role in the contraction phase.

To confirm that the increased accumulation of influenza virus-specific CD8 T cells was not due to an increase or persistence of the viral antigen, we compared the kinetics of viral load in the lungs of infected WT, IFN-γ$^{-/-}$, and IFN-γR$^{-/-}$ mice by using the standard plaque assay. By the results of this assay, we saw that there was no effect on viral titers or rates of viral clearance in the absence of IFN-γ or IFN-γR (Fig. 1E). We could not detect any virus in the lungs on day 8 p.i. by using the plaque assay. As this assay is limited in sensitivity, we measured mRNA of the viral M protein in the infected lungs by quantitative RT-PCR analysis until day 14 p.i. Although we could detect viral RNA until about day 10, we did not observe any differences in the copy numbers of viral RNA between the WT, IFN-γ$^{-/-}$, and IFN-γR$^{-/-}$ mouse lungs (Fig. 1F). Hence, increased viral titers were not responsible for the increased CD8 T cell numbers in the absence of IFN-γ signaling. To confirm that viral clearance coincided with functional antigen disappearance *in vivo*, we isolated dendritic cells (DCs) from lungs and lung draining lymph nodes of WT, IFN-γ$^{-/-}$, and IFN-γR$^{-/-}$ mice infected with PR/8-OT-1 (PR/8 virus containing SIINFEKL within the virus NA stalk) at various time points to see if they could stimulate CD8 T cell proliferation. The extent of DC-mediated priming of OT-1 CD8 T cells would thus serve as a surrogate readout of viral antigen levels within the lung. DCs isolated from mice at day 5 p.i. strongly stimulated proliferation of the OT-1 CD8 T cells. In contrast, we did not observe significant proliferation of OT-1 cells with DCs isolated at day 11 p.i. These results confirm the disappearance of functional antigen by day 11 p.i. in WT, IFN-γ$^{-/-}$, and IFN-γR$^{-/-}$ mice (data not shown), which correlates well with RT-PCR results for viral mRNA. These data demonstrate that the increased CD8 T cell numbers in the absence of IFN-γ signaling are not due to increased viral titers or extended antigen presentation.

Contraction of antigen-specific CD8 T cell response in IFN-γ$^{-/-}$ and IFN-γR$^{-/-}$ mice. Given that no decrease in the number of antigen-specific CD8 T cells was evident in the lungs of the IFN-γ$^{-/-}$ and IFN-γR$^{-/-}$ mice following the peak of the response, we hypothesized that this was due to the absence of an efficient contraction phase. Hence, we examined whether IFN-γ regulates the contraction of antigen-specific CD8 T cells at a time point when influenza virus infection is completely resolved and the lungs have returned to a normal state. Virus-specific CD8 T cells in the lungs and BAL fluid of WT, IFN-γ$^{-/-}$, and IFN-γR$^{-/-}$

mice were quantified on day 28 p.i., a time point at which the antigen-specific CD8 T cell numbers in the lung would have been reduced substantially following the death of a large number of effector cells. Although there were considerable decreases in the numbers of NP_{366}^+ CD8 T cells in the BAL fluid (Fig. 2A) and lungs (Fig. 2B) of the WT mice, we could still observe significantly larger numbers of these cells in the IFN-γ$^{-/-}$ and IFN-γR$^{-/-}$ mice (Fig. 2A and B). Thus, we concluded that there was an abnormal contraction of virus-specific CD8 T cells in the lungs of IFN-γ$^{-/-}$ mice and IFN-γR$^{-/-}$ mice. This was also true of the spleens of these animals (Fig. 2C), indicating that this is not only a localized phenomenon. We also observed significantly larger numbers of NP_{366}^+ CD8 T cells in the lungs of the IFN-γ$^{-/-}$ mice and IFN-γR$^{-/-}$ mice on day 120 p.i. (Fig. 2D). Since our results with PR/8 were different from what was observed in an earlier study with a different strain of influenza virus, A/HKx31 (X31), we performed the experiment with X31 to evaluate whether differences in viral strains could explain the observed differences between these studies. However, our observations were consistent between PR/8 and X31 infections, and we observed similar phenotypes in mice infected A/HKx31 on day 28 p.i. (Fig. 3A to C) and day 120 p.i. (Fig. 3D and E).

Increased accumulation of antigen-specific CD8 T cells in the absence of IFN-γ is linked to increased apoptosis in influenza virus-specific CD8 T cells. We measured the rates of proliferation of CD8 T cells in the presence or absence of IFN-γ. Our data indicated that IFN-γ deficiency did not alter the proliferation of the CD8 T cells (data not shown). We also did not observe any difference in the precursor frequencies of the NP_{366}^+ CD8 T cells in the spleens and pooled lymph nodes of uninfected IFN-γ$^{-/-}$ mice and IFN-γR$^{-/-}$ mice compared to WT mice (data not shown). The increased accumulation of virus-specific CD8 T cells could also be explained by a decrease in rates of cell death. To determine if IFN-γ could influence cell death, we measured the number of live cells in cultures of IFN-γ$^{-/-}$ CD8 T cells after stimulation in the presence or absence of increasing amounts of recombinant IFN-γ (rIFN-γ). We observed a dose-dependent decrease in the number of surviving cells 48 h after culture with rIFN-γ (Fig. 4A). We also observed an increase in the number of surviving WT cells when IFN-γ signaling was blocked with antibodies to both IFN-γ and IFN-γR simultaneously (Fig. 4B). These data suggested that IFN-γ could cause an increased death rate in CD8 T cells during an immune response. To determine whether the CD8 T cells from the influenza virus-infected IFN-γ$^{-/-}$ mice had decreased apoptosis, we stained freshly isolated CD8 T cells from the lungs of WT and IFN-γ$^{-/-}$ mice for annexin V and 7-AAD at day 12 post-influenza virus infection, just after the peak of the response. We observed that an increased percentage of NP_{366}^+ cells from WT mice stained positive for annexin V and 7-AAD compared to IFN-γ$^{-/-}$ mice (Fig. 4C). This was true of late apoptotic, annexin V$^+$ 7-AAD$^+$ NP_{366}^+ cells (Fig. 4D) and all annexin V$^+$ NP_{366}^+ cells (Fig. 4E). We next examined whether the addition of exogenous IFN-γ to antigen-specific CD8 T cells from IFN-γ$^{-/-}$ mice would result in enhanced cell death. Lung lymphocytes enriched from IFN-γ$^{-/-}$ mice infected with 5 PFU of PR8 influenza virus were harvested on day 14 p.i. and cultured for 24 h in the presence or absence of rIFN-γ. After 24 h, the cells were stained with antibodies against CD3, CD8, and NP_{366} pentamer, and the numbers of live cells (7-AAD$^-$) were enumerated. Addition of rIFN-γ to the cell cultures resulted in a decrease in the
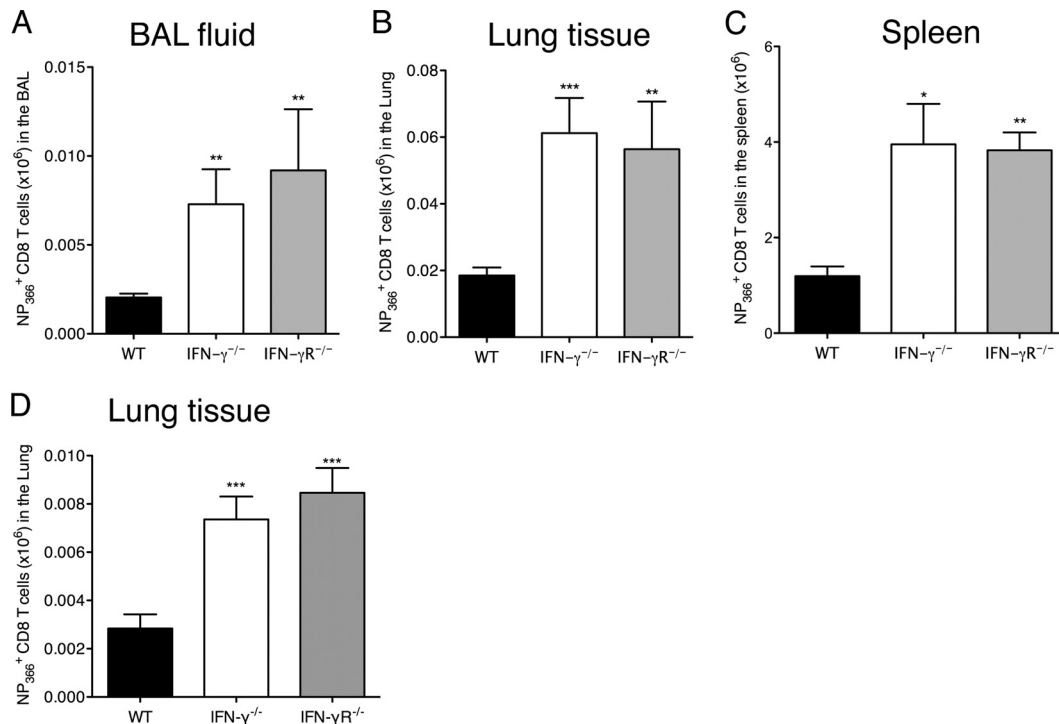
FIG 2 Reduced contraction of antigen-specific CD8 T cell responses and increased memory precursor cell compartment in IFN-$\gamma^{-/-}$ and IFN-γR$^{-/-}$ mice after influenza virus infection. C57BL/6 WT, IFN-$\gamma^{-/-}$, and IFN-γR$^{-/-}$ mice were infected with 5 PFU of influenza A/PR/8/34 virus. NP$_{366}^+$ CD8$^+$ T cell numbers were examined in the BAL fluid (A), lung tissue (B), and spleen (C) on day 28 p.i. and in the lung tissue on day 120 p.i. (D). The numbers of CD8$^+$ NP$_{366}^+$ cells (means $\pm$ SEM) shown were calculated from the total counts and the percentages of cells staining positive. *, $P < 0.05$; **, $P < 0.01$; ***, $P < 0.001$ (determined using Student's t test). Data are representative of at least 3 independent experiments with 4 or 5 mice per group.

percentage of live NP$_{366}^+$ CD8 T cells from the IFN-$\gamma^{-/-}$ cultures (Fig. 4F and G). This effect was specifically seen in antigen-specific CD8 T cells but not on other cell types (data not shown). This confirmed our hypothesis that IFN-γ regulates CD8 T cell survival and induces cell death in antigen-specific CD8 T cells.

The absence of IFN-γ signaling and increased influenza virus-specific CD8 T cell numbers do not alter the extent of lung damage due to a sublethal influenza virus infection. We next evaluated whether the increased CD8 T cell numbers contributed to increased lung damage in mice in the absence of IFN-γ signaling. We first looked at pulmonary histopathology in lung sections of WT, IFN-$\gamma^{-/-}$, and IFN-γR$^{-/-}$ mice at different time points after influenza virus infection (Fig. 5A). Before the infection, the lung sections of all the mice looked normal. By day 3 p.i., all mice exhibited similar extents of inflammatory cell infiltration into the airways, which increased significantly by day 7 p.i. Partial resolution of inflammation was seen by day 14 p.i. These histological findings suggest that the absence of IFN-γ signaling does not alter the level of lung damage post-influenza virus infection (Fig. 5B). We next examined albumin leakage into the BAL fluid as an indicator of lung damage (Fig. 5C). Although we did not observe any changes after 8 days, we observed slightly increased levels of albumin leakage in the BAL fluid of WT mice compared to IFN-$\gamma^{-/-}$ mice on days 11 and 14, indicating that there may be decreased inflammation in the absence of IFN-γ signaling later in the infection. We concluded that the lack of IFN-γ did not affect lung pathology, and although there was an abnormal contraction of CD8 T cells in the

IFN-$\gamma^{-/-}$ mice, this did not exacerbate the immunopathology due to influenza virus infection.

IFN-γ deficiency does not alter effector function of antigen-specific CD8 T cells. Next, we assessed the effector function of influenza virus-specific CD8 T cells at different points in the response. We first measured the ability of the NP$_{366}^+$ CD8 T cells from the lungs of infected mice to produce cytokines by intracellular cytokine staining *ex vivo*. There were no differences in the production of cytokines such as IL-2 and tumor necrosis factor alpha (TNF-α) by the NP$_{366}^+$ CD8 T cells from WT, IFN-$\gamma^{-/-}$, and IFN-γR$^{-/-}$ mice (Fig. 6A and B). We further examined the cytotoxic potential of these cells by using a chromium release assay. CD8 T cells from lungs of infected mice were tested for lysis of ^{51}Cr-labeled EL-4 target cells pulsed with NP$_{366}$ peptide. The background cytotoxicity of non-peptide-pulsed EL-4 cells was subtracted to calculate peptide-specific cytotoxicity. The CD8 T cells isolated from the lungs of WT, IFN-$\gamma^{-/-}$, and IFN-γR$^{-/-}$ mice showed no significant differences in cytotoxicity. This was true for day 7 p.i. (Fig. 6C) and day 11 p.i. (Fig. 6D). These results confirm that antigen-specific CD8 T cells show similar cytotoxicities in the absence of IFN-γ signaling.

IFN-γ deficiency increases the size of the memory precursor cell compartment in the lung as observed by proportion of IL-7R$^+$ cells. In view of the fact that there was enhanced survival of antigen-specific CD8 T cells in the IFN-$\gamma^{-/-}$ and IFN-γR$^{-/-}$ mice during the contraction phase, we hypothesized that these cells might be memory cell precursors. We characterized the expression of receptors for key cytokines that regulate T cell survival
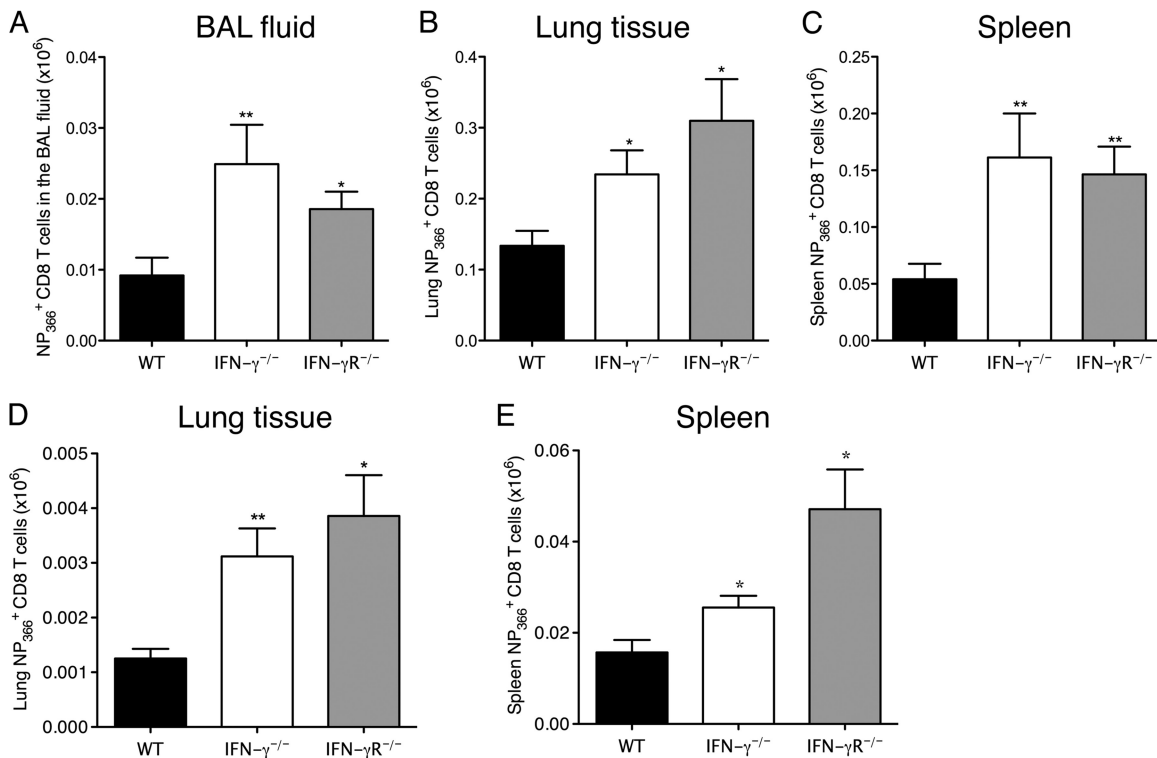
FIG 3 Increased numbers of antigen-specific CD8 T cells in IFN-$\gamma^{-/-}$ and IFN-$\gamma R^{-/-}$ mice after HKx31 infection. C57BL/6 WT, IFN-$\gamma^{-/-}$, and IFN-$\gamma R^{-/-}$ mice were infected with 50,000 PFU of influenza A/HK/x31 virus. $NP_{366}{}^+$ CD8$^+$ T cell numbers were examined in the BAL fluid (A), lung tissue (B), and spleens (C) of the mice on day 28 p.i. and in the lung tissue (D) and spleens (E) on day 120 p.i. The numbers of CD8$^+$ $NP_{366}{}^+$ cells (means ± SEM) shown were calculated from the total counts and the percentages of cells staining positive. *, $P < 0.05$; **, $P < 0.01$ (determined using Student's t test). Data are representative of at least 2 independent experiments with 4 or 5 mice per group.

and differentiation into memory cells, namely, IL-2R (α CD25, β CD122, and γ CD132), IL-7R (α CD127 and γ CD132), and IL-15R (α CD215, β CD122, and γ CD132) on the surfaces of the $NP_{366}{}^+$ CD8 T cells at the peak of the CD8 T cell response (Fig. 7A). We observed no differences in the expression of CD25, CD132, and CD215 and only slight differences in CD122 expression. Most notably, we observed significant differences in the levels of CD127 (IL-7Rα) expression. The increased expression of IL-7Rα on CD8 T cells at the peak of the CD8 T cell response is known to identify the effector CD8 T cells that will differentiate into memory cells (25). Accordingly, we examined the expression of IL-7Rα on the antigen-specific CD8 T cells among WT, IFN-$\gamma^{-/-}$, and IFN-$\gamma R^{-/-}$ CD8 T cells at the peak of the CD8 T cell response, i.e., day 11 p.i. (Fig. 7B and C). We found that in the WT mice, only about 3 to 7% of the $NP_{366}{}^+$ CD8 T cells expressed IL-7Rα, which is consistent with the predicted percentage of cells that survive to become long-lived memory cells. Surprisingly, in IFN-$\gamma^{-/-}$ and IFN-$\gamma R^{-/-}$ mice, we observed that significantly higher percentages ($\sim$10 to 15%) of the antigen-specific CD8 T cells expressed IL-7Rα at this point (Fig. 7B and C). This observation is consistent with our previous results, which show that more antigen-specific CD8 T cells survive in these mice. Hence, we concluded that in the absence of IFN-γ signaling, a larger number of memory precursor cells are formed. We examined expression of IL-7Rα on day 14 (Fig. 7B and D) after infection. Although the percentage of cells expressing IL-7Rα on day 14 was higher, the difference between WT mice and the IFN-$\gamma^{-/-}$ and IFN-$\gamma R^{-/-}$

mice was maintained. These data suggest that IFN-γ controls the survival of antigen-specific CD8 T cells by regulating the expression of IL-7Rα during the contraction phase to promote death of effector CD8 T cells.

We also looked at the levels of intracellular Bcl-2 expressed by the antigen-specific IL-7R^{hi} and IL-7R^{lo} cells (Fig. 7E and F) and observed that the IL-7R^{hi} cells expressed higher levels of the anti-apoptotic molecule Bcl-2, indicating that these cells are more refractive to apoptosis and hence may be long-lived memory precursors. To confirm whether IL-7R expression was indeed key to the survival of the influenza virus-specific CD8 T cells *in vivo*, we delivered IL-7 neutralizing antibody or control isotype IgG to the lungs of infected WT and IFN-$\gamma^{-/-}$ mice on day 11 p.i. by the intranasal route and quantified the $NP_{366}{}^+$ CD8 T cells in the lung tissues of the treated mice on day 14 p.i. Blocking IL-7 enhanced the cell death of the $NP_{366}{}^+$ CD8 T cells, and significantly fewer cells survived in the lungs of the IFN-$\gamma^{-/-}$ mice than in the control-treated IFN-$\gamma^{-/-}$ mice (Fig. 7G). Even fewer $NP_{366}{}^+$ CD8 T cells survived in the lungs of WT mice treated with anti-IL-7. This finding demonstrates that IL-7R expression on $NP_{366}{}^+$ CD8 T cells is functionally important in their survival during the contraction phase. Hence, the increased frequency of IL-7R (CD127) on $NP_{366}{}^+$ CD8 T cells in the absence of IFN-γ signaling enhances their survival and, consequently, their ability to develop into memory cells.

IFN-γ deficiency does not affect the distribution of memory CD8 T cells in the effector memory (CD44^{hi} CD62L^{lo}) and central memory (CD44^{hi} CD62L^{hi}) T cells. The magnitude of the
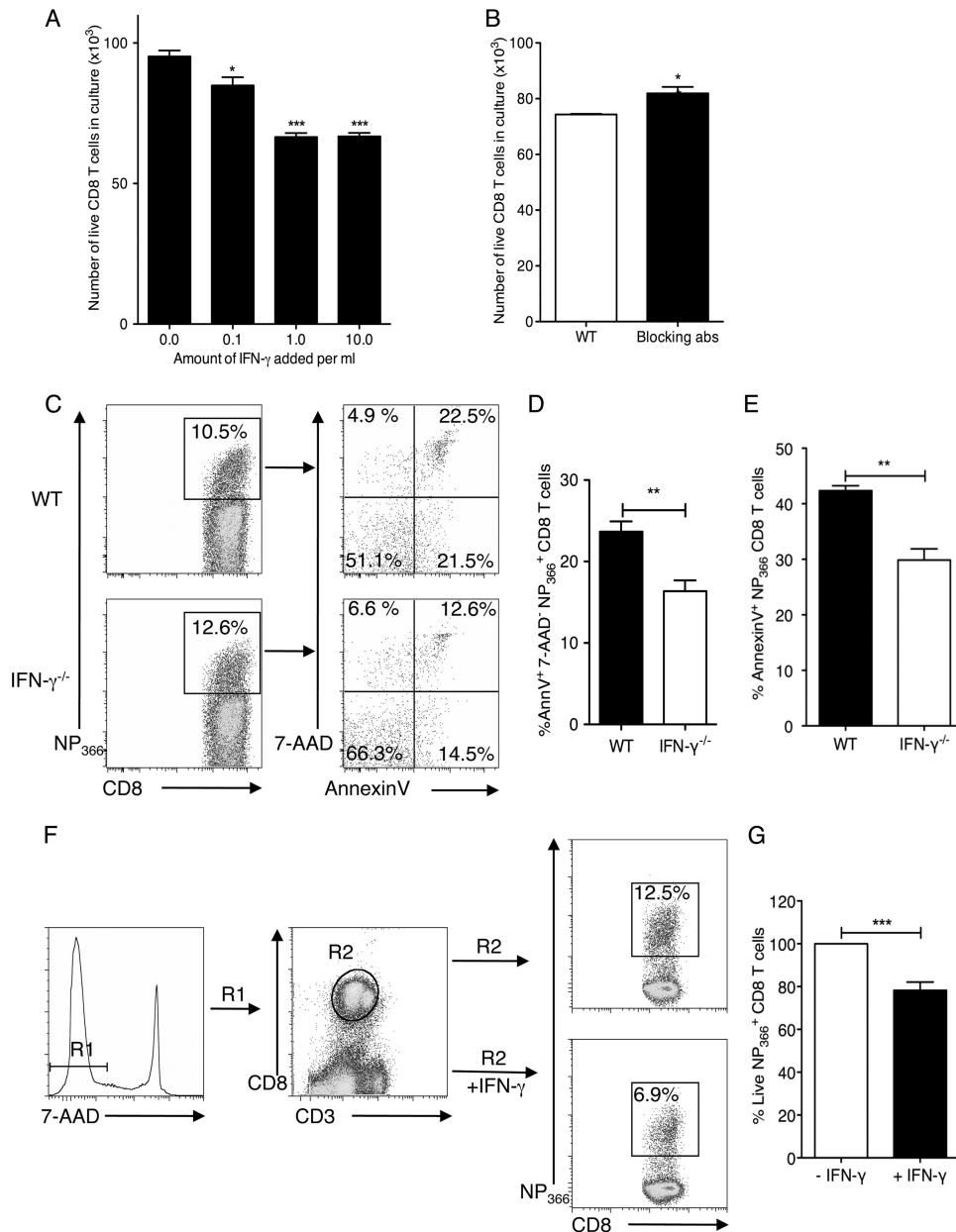
FIG 4 The presence of IFN-γ leads to decreased CD8 T cell survival in culture and in influenza virus-specific CD8 T cells in the lungs of infected mice. CD8 T cells were purified from the spleens and lymph nodes of WT and IFN-γ$^{-/-}$ mice. IFN-γ$^{-/-}$ CD8 T cells were stimulated *in vitro* with phorbol myristate acetate (PMA) and ionomycin and cultured in the absence or presence of increasing amounts of recombinant IFN-γ in culture for 48 h. (A) Cells were stained with anti-CD3 and anti-CD8 antibodies and with 7-AAD. Live cells (7-AAD negative) were counted in all cultures and plotted. (B) WT CD8 T cells were stimulated in the presence or absence of blocking antibodies to IFN-γ and IFN-γR1 for 48 h. Live cells were counted and plotted after 48 h. (C) C57BL/6 WT or IFN-γ$^{-/-}$ mice were infected with 5 PFU of influenza A/PR/8/34 virus, and lungs were harvested on day 12 p.i. The CD8^{+} T cells from the lungs were isolated and stained with annexin V and 7-AAD. Representative flow cytometry plots of annexin V and 7-AAD staining of WT and IFN-γ$^{-/-}$ mice are shown. (D and E) The percentages of cells positive for annexin V and 7-AAD (D) or annexin V only (E) were plotted. (F) IFN-γ$^{-/-}$ mice were infected with 5 PFU of influenza A/PR/8/34 virus, and CD8^{+} T cells were harvested on day 14 p.i. The Ficoll-enriched cells were cultured in the presence or absence of rIFN-γ for 24 h. Live NP$_{366}$$^{+}$ CD8^{+} T cell proportions were examined in the culture according to the gating strategy. (G) The NP$_{366}$$^{+}$ CD8^{+} T cells in the cultures without IFN-γ were considered to represent 100%, and the percentage of live NP$_{366}$$^{+}$ CD8^{+} T cells in the cultures with IFN-γ were calculated accordingly. Means ± SEM are shown and were calculated from the percentages of cells staining positive. Data are representative of two or three independent experiments. *, $P < 0.05$; **, $P < 0.01$; ***, $P < 0.001$.

memory cell pool is a function of the rates of expansion and contraction of the CD8 T cell response. To investigate this, we examined the phenotypic features of the antigen-specific CD8 T cell memory pool on day 120 p.i. The distribution of T$_{CM}$ or central

memory CD8 T cell (CD44^{hi} CD62L^{hi}) and T$_{EM}$ or effector memory CD8 T cell (CD44^{hi} CD62L^{low}) frequencies was not affected at the site of infection (Fig. 8A). This was reflected in the total numbers of antigen-specific effector memory CD8 T cells in the lung,
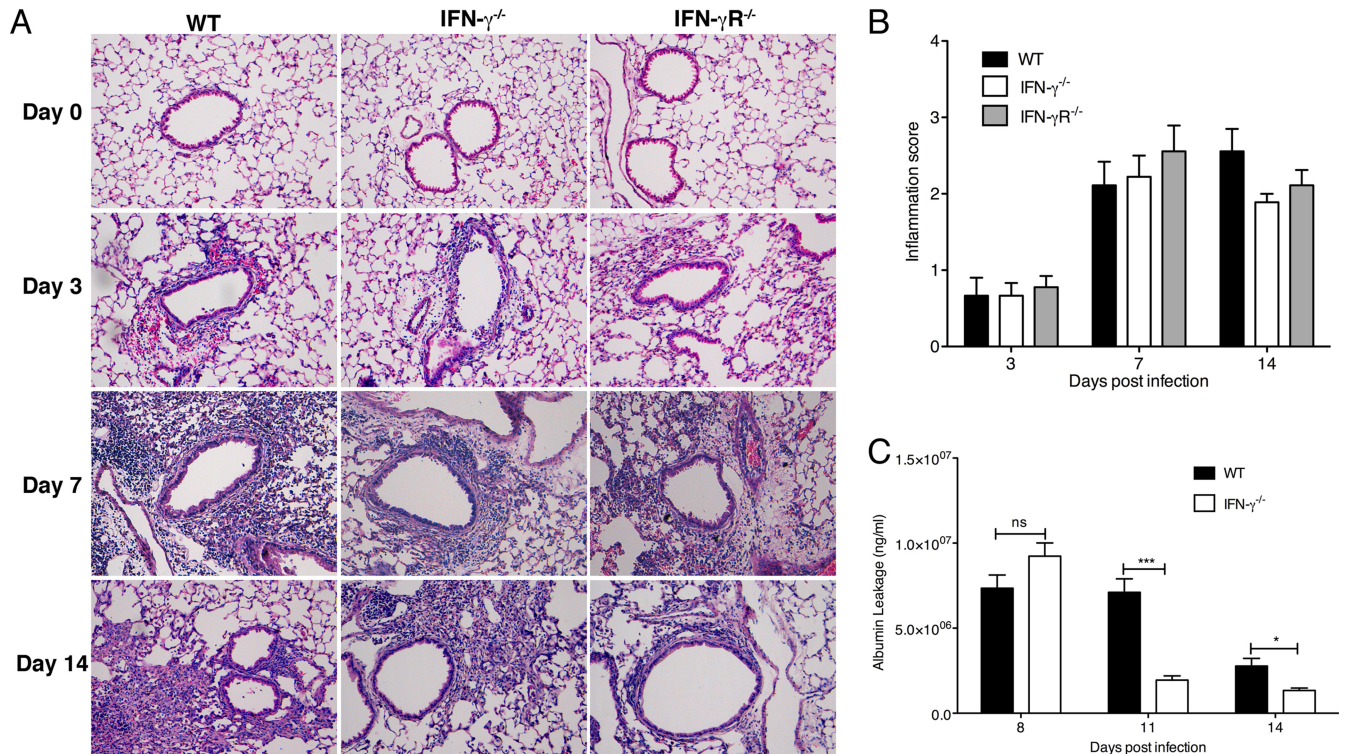
FIG 5 IFN-γ or IFN-γR deficiency does not lead to changes in lung damage following a 5-PFU influenza virus infection. (A) C57BL/6 WT, IFN-γ$^{-/-}$, and IFN-γR$^{-/-}$ mice were infected with 5 PFU of influenza A/PR/8/34 virus, and the lungs were perfused and harvested before infection (day 0) or on day 3, 7, or 14 p.i. for hematoxylin and eosin (H&E) staining. Representative images of the H&E sections are shown. (B) The lung sections were scored blind by using a 5-point scoring system as follows: 0, no infiltrating cells; 1, only 1 or 2 airways or vessels have cell infiltration (<3 cells deep); 2, 25 to 50% of the whole section has inflammation (>3 cells deep); 3, 50 to 75% of the whole section has inflammation (>3 cells deep); and 4, >75% of the whole section has inflammation (>3 cells deep). Multiple lung sections were scored per lung, with 3 lungs scored per group per time point, and the means ± SEM were plotted. (C) Albumin leakage into the BAL fluid of infected mice was measured using enzyme-linked immunosorbent assay (ELISA) at days 8, 11, and 14 p.i. Means ± SEM are plotted. *, $P < 0.05$; ***, $P < 0.001$ (determined using Student's t test). Data are pooled from two to three experiments with 4 or 5 mice per group.

which were equally increased in both memory cell compartments in the absence of IFN-γ signaling (Fig. 8B), indicating that IFN-γ did not affect distribution of the memory cell compartments.

Enhanced secondary CD8 T cell responses in IFN-γ$^{-/-}$ and IFN-γR$^{-/-}$ mice after a heterologous virus challenge. In order to confirm that the increased frequencies of IL-7Rα-expressing cells in the absence of IFN-γ signaling were indeed memory precursor cells, we compared the recall responses in these mice after a secondary challenge with a heterologous strain of influenza virus. For this set of experiments, mice were infected with HKx31 (H3N2) and then reinfected after 30 to 35 days with PR/8. Strain HKx31 (H3N2) has the same internal proteins as PR/8 but has different hemagglutinin and neuraminidase proteins on the surface. All the HKx31-infected mice were completely protected from the rechallenge with PR/8. As expected for a recall response, we observed an earlier CD8 response and higher frequencies of antigen-specific CD8 T cells in the lungs of the infected mice than those observed with a primary infection. However, the differences between the CD8 responses of WT, IFN-γ$^{-/-}$, and IFN-γR$^{-/-}$ mice were greatly enhanced after the secondary challenge, as the NP$_{366}$$^+$ CD8 T cells accounted for ~30% of the CD8 T cells in the WT mice, but in the IFN-γ- and IFN-γR-deficient mice, these cells accounted for >50% of the CD8 T cells (Fig. 8C). There was also a dramatic difference in the total number of NP$_{366}$$^+$ CD8 T cells in IFN-γ$^{-/-}$ compared to WT mice (Fig. 8D). This experi-

ment was repeated with reinfection after 120 days p.i., with similar results (data not shown). Finally, when we examined the kinetics of lung viral RNA by qRT-PCR, we observed high viral titers in the lungs of mice with a primary infection of 500 PFU PR/8, whereas all reinfected mice showed much lower titers. Similar to primary infection with a low dose of 5 PFU PR/8 (Fig. 1F), there was no difference in viral load between the WT, IFN-γ$^{-/-}$, and IFN-γR$^{-/-}$ mice after infection with a high dose of influenza virus (Fig. 8F). In the reinfected mice, however, we saw that the levels of viral RNA in the lungs of the IFN-γ$^{-/-}$ and IFN-γR$^{-/-}$ mice were significantly reduced compared to those in WT mice on day 8 after reinfection. This demonstrates that persisting antigen-specific CD8 T cells in IFN-γ$^{-/-}$ and IFN-γR$^{-/-}$ mice after resolution of the primary infection do indeed lead to higher frequencies of memory precursors and hence produce better recall responses and better viral resolution in the absence of IFN-γ signaling.

In summary, our data suggest that gamma interferon regulates the magnitude of influenza virus-specific CD8 T cell responses influencing the generation of the memory population, with no obvious loss in effector function.

DISCUSSION

Understanding the immune response to infection and the specific interactions between the virus and the host is fundamental to the development of better vaccine strategies. This is especially true for
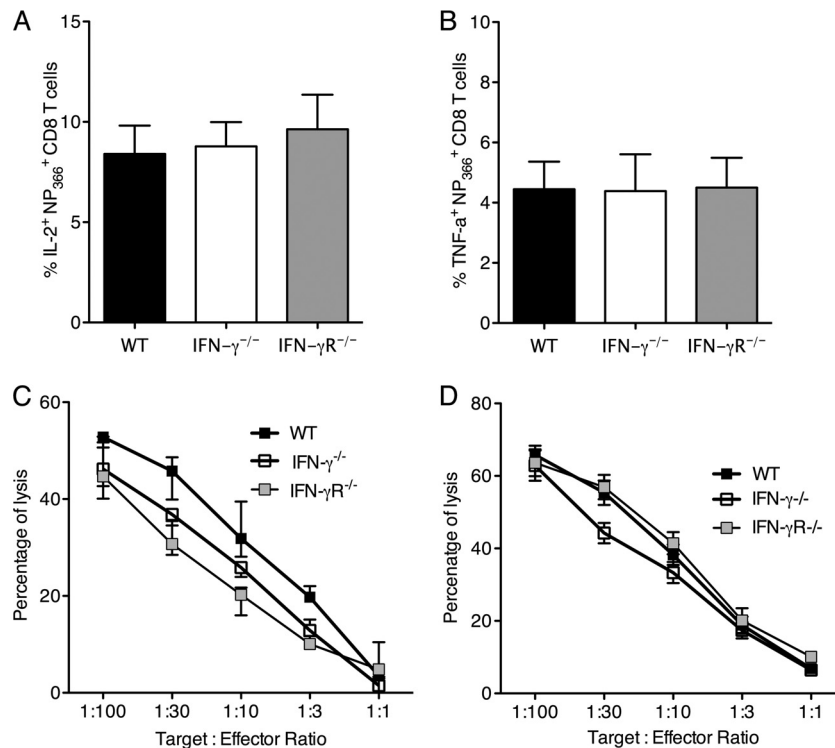
FIG 6 IFN-γ deficiency does not affect the effector function of antigen-specific CD8 T cells after influenza virus infection. C57BL/6 WT, IFN-γ$^{-/-}$, and IFN-γR$^{-/-}$ mice were infected with 5 PFU of influenza A/PR/8/34 virus, and the percentages of NP$_{366}^+$ CD8 T cells expressing IL-2 (A) and TNF-α (B) on day 8 p.i. were measured. Cytotoxic profiles are shown for CD8 T cells from the lung on day 7 (C) and day 11 (D) p.i., determined by ^{51}Cr release assay and expressed as percentages of specific lysis of target cells. Data are representative of at least 3 independent experiments with 4 or 5 mice per group.

influenza vaccines, as current strategies lack the ability to elicit lasting CD8 T cell memory responses. In the present study, we show for the first time that IFN-γ–IFN-γR signaling plays a key role in the modulation of antigen-specific CD8 T cell contraction and memory development in response to influenza virus infection. We showed that in the absence of IFN-γ signaling, the contraction phase of the CD8 T cell responses was aberrant, resulting in the accumulation of antigen-specific CD8 T cells for as long as 120 days p.i., when the responses in WT mice had declined significantly. IFN-γ directly regulated effector CD8 T cell survival, as we could induce cell death in IFN-γ$^{-/-}$ effector cells by culturing them in the presence of rIFN-γ. In addition, larger proportions of antigen-specific CD8 T cells in IFN-γ$^{-/-}$ and IFN-γR$^{-/-}$ mice expressed IL-7Rα, which is functionally important for survival of effector cells during the contraction phase of the response. In a recall response to secondary challenge with a heterologous strain of influenza virus, larger numbers of influenza virus-specific CD8 T cells were found in the IFN-γ$^{-/-}$ and IFN-γR$^{-/-}$ mice than in WT mice, confirming that higher frequencies of memory precursors are indeed formed in the absence of IFN-γ signaling, which subsequently confer the ability to clear virus faster than in WT mice.

Gamma interferon is known to influence the rate of proliferation and apoptosis in activated T cells (26–28). Therefore, we thought that the increased accumulation of antigen-specific CD8 T cells in the lungs of influenza virus-infected IFN-γ$^{-/-}$ and IFN-γR$^{-/-}$ mice could be a result of the rates of cell proliferation and/or death. However, analysis of in vitro and in vivo proliferation indicated that IFN-γ deficiency did not alter the rate of pro-

liferation of CD8 T cells but, instead, affected CD8 T cell survival. Furthermore, we observed decreased rates of cell death in antigen-specific CD8 T cells in the IFN-γ$^{-/-}$ mice. Cell death could also be induced in antigen-specific CD8 T cells by the addition of rIFN-γ to ex vivo cultures. This mechanism is consistent with findings from other studies which show that IFN-γ contributes to activation-induced cell death of in vitro-activated T cells (26, 29).

We hypothesized that homeostatic cytokine receptors may be expressed differentially in the absence of IFN-γ signaling and hence responsible for increased rates of survival of CD8 T cells in the IFN-γ- and IFN-γR-deficient mice. Studies in LCMV showed that IFN-γ had an effect on expression of IL-7R (19). Also, expression of IL-7Rα (CD127) on antigen-specific CD8 T cells at the peak of the response is known to identify cells that will survive the contraction phase to give rise to memory precursor populations (25). We observed that IFN-γ influenced the levels of IL-7R expression on effector CD8 T cells during an influenza virus infection. IL-7 is a homeostatic cytokine which delivers survival signals to CD8 T cells by inhibiting apoptosis; IL-7 increases the levels of anti-apoptotic molecules such as Bcl-2 (25). We found that this was also true for influenza virus and observed increased frequencies of cells expressing IL-7Rα at the peak of the response in the absence of IFN-γ signaling, and we showed that these cells also expressed higher levels of Bcl-2. This agreed with our initial finding that increased numbers of cells survived the contraction phase in the absence of IFN-γ signaling. We confirmed that expression of IL-7R was functionally significant by blocking IL-7 in vivo. Neutralizing IL-7 in the IFN-γ-deficient mice reduced the numbers of influenza virus-specific CD8 T cells to WT levels. Hence,
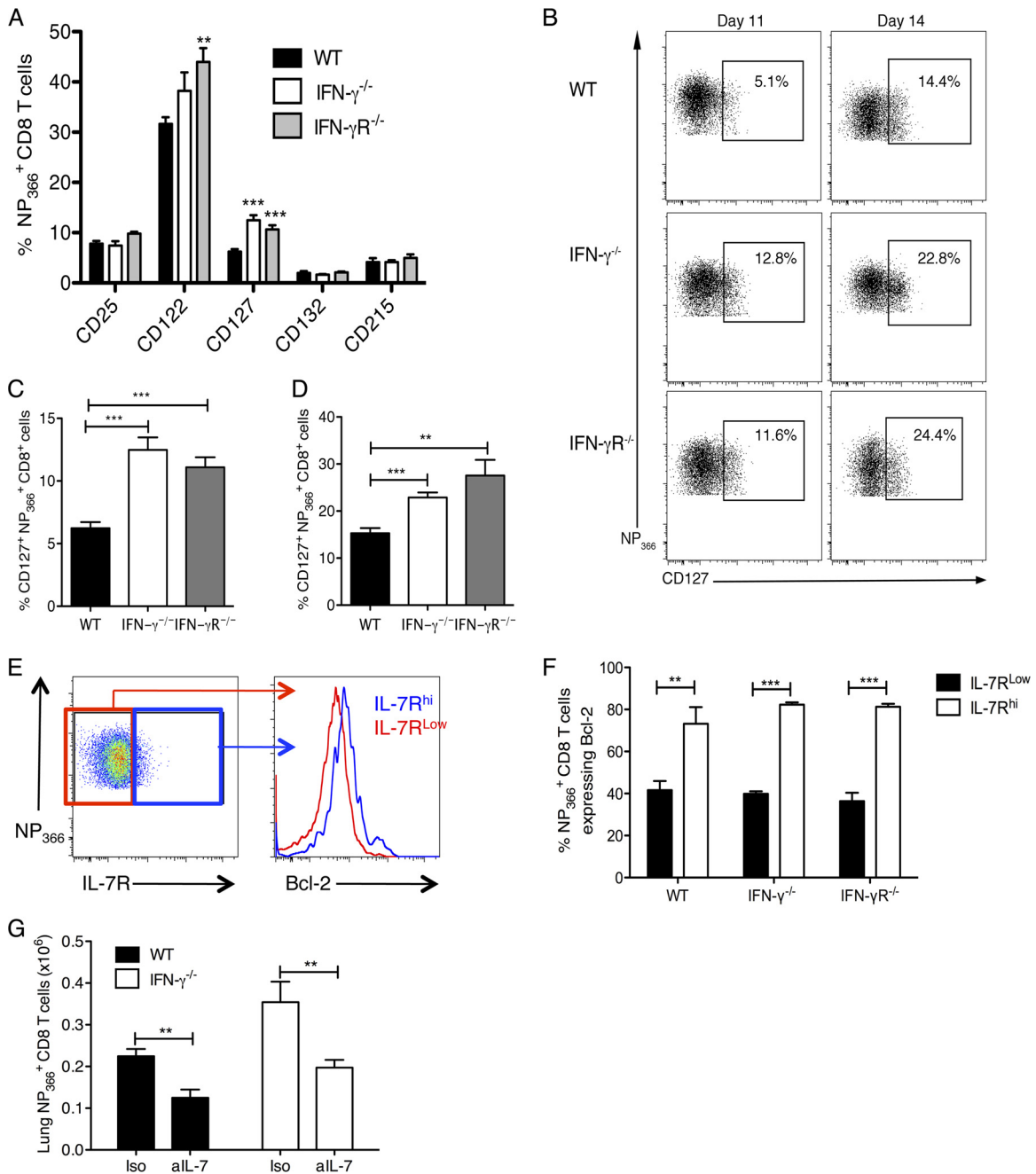
FIG 7 Increased memory precursor CD8 T cells in the lungs of IFN-γ$^{-/-}$ and IFN-γR$^{-/-}$ mice. NP$_{366}$$^+$ CD8$^+$ T cell proportions were examined in the lung tissue for expression of different receptors on day 11 p.i. (A) Graphs showing the percentages of NP$_{366}$$^+$ CD8$^+$ T cells in the lung expressing the receptor subunits for IL-2 (CD25, CD122, and CD132), IL-7 (CD127 and CD132), and IL-15 (CD215 and CD132) on day 11 p.i. (B to D) Representative flow cytometry plots (B) and graphs (C and D) showing the percentages of cells expressing IL-7Ra in the WT, IFN-γ$^{-/-}$, and IFN-γR$^{-/-}$ mice on day 11 p.i. (C) and day 14 p.i. (D). Cells were stained with anti-CD3 and anti-CD8 antibodies, the H2-D^b NP$_{366}$ tetramer, and antibodies to the respective receptors on the indicated days. (E) Representative flow cytometry plots showing levels of Bcl-2 in the IL-7R^{hi} and IL-7R^{lo} populations of antigen-specific CD8 T cells. (F) Graph showing percentages of IL-7R^{low} and IL-7R^{hi} NP$_{366}$ CD8 T cells expressing Bcl-2. (G) Infected WT and IFN-γ$^{-/-}$ mice were treated intranasally with 0.05 mg anti-IL-7 polyclonal antibody (PAb) (aIL-7) or control isotype goat IgG (Iso) on day 11 p.i., and NP$_{366}$$^+$ CD8 T cells were enumerated in the lungs of these mice on day 14 p.i. Data were pooled from two or three independent experiments with 4 or 5 mice/group/experiment. **, $P < 0.01$; ***, $P < 0.001$ (determined using Student's t test).

the higher expression level of IL-7R is the reason that more cells in these mice are resistant to cell death and thus survive the contraction phase to form a larger percentage of memory cells. In addition to IL-7Rα, other molecules may also regulate the survival of these cells, and further studies will be needed to identify the factors responsible.

Antigen-specific CD8 T cells in IFN-γ$^{-/-}$ and IFN-γR$^{-/-}$ mice exhibited more IL-7Rα expression at the peak of expansion, and their numbers did not contract compared with antigen-specific CD8 T cells in WT mice. However, it remains to be determined if early IFN-γ signals in T cells directly regulate which effector cells will or will not upregulate IL-7Rα. Thus, determining
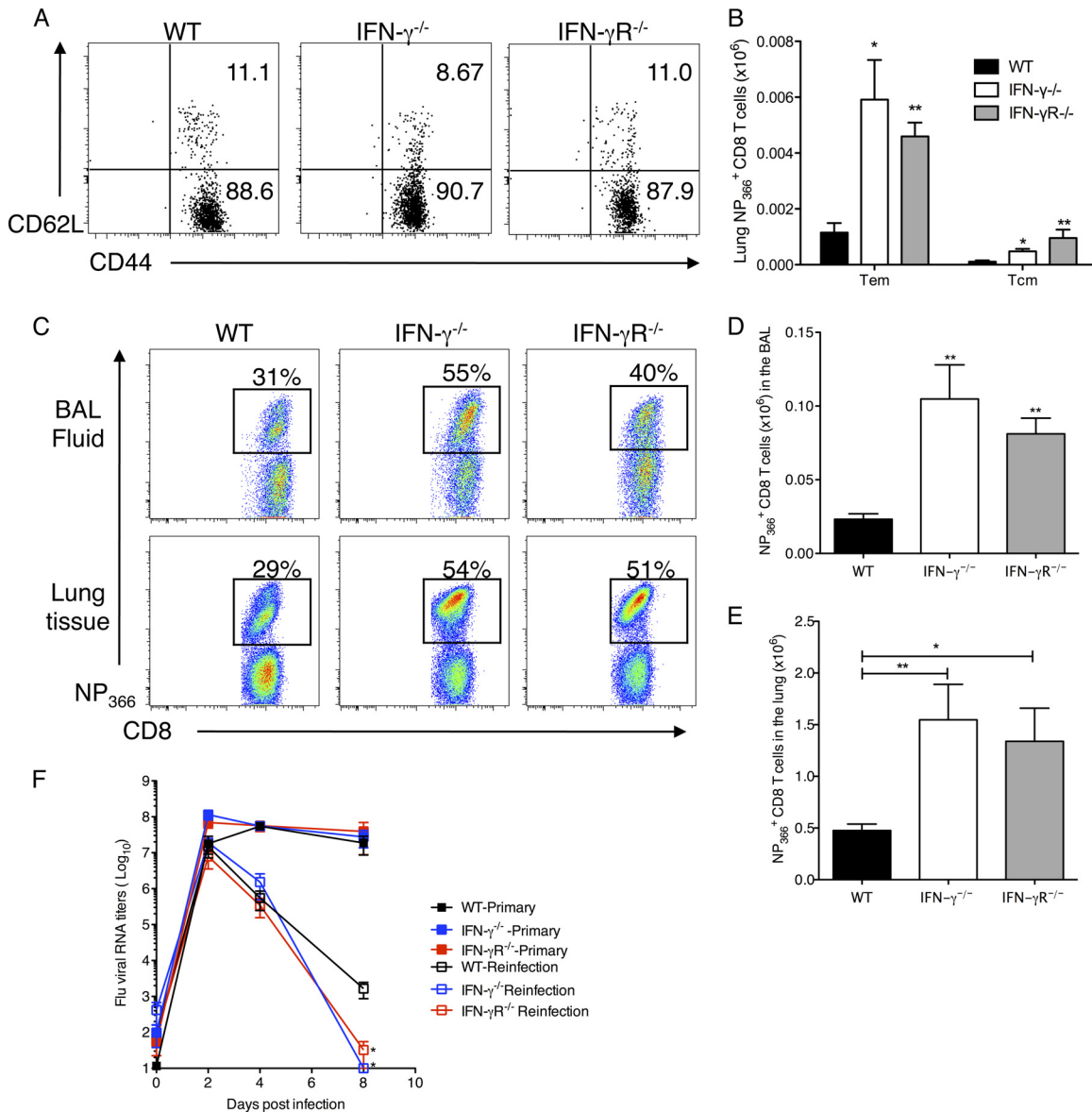
FIG 8 Unaltered distribution of memory T cell subsets and enhanced secondary CD8 T cell responses in IFN-$\gamma^{-/-}$ and IFN-γR$^{-/-}$ mice after heterologous challenge. (A) NP$_{366}^+$ CD8$^+$ T cells in the lung tissue of mice were examined on day 120 p.i. for their expression of CD44 and CD62L. Representative flow cytometry plots are shown. (B) Numbers of effector memory (CD44^{hi} CD62L^{lo}) and central memory (CD44^{hi} CD62L^{hi}) CD8$^+$ NP$_{366}^+$ cells (means ± SEM) were calculated from the total counts and the percentages of cells staining positive in the lungs of infected mice. For rechallenge experiments, C57BL/6 WT, IFN-$\gamma^{-/-}$, and IFN-γR$^{-/-}$ mice were infected with a sublethal dose of influenza HK/x31 virus (H3N2), and after 30 days, mice were infected with a second virus, A/PR/8/34 (H1N1), and monitored for 8 days after infection. (C) Representative flow cytometry plots of the proportions of NP$_{366}^+$ CD8$^+$ T cells in the BAL fluid and lung tissue of mice reinfected with 500 PFU of PR/8. Cells were gated on CD3$^+$ CD8$^+$ T cells. Numbers represent percentages of CD8$^+$ T cells which are also NP$_{366}^+$. (D and E) Total NP$_{366}^+$ CD8$^+$ T cell numbers in the BAL fluid (D) and lung tissue (E) on day 8 after reinfection. The number of NP$_{366}^+$ CD8$^+$ cells (means ± SEM) shown were calculated from the total counts and the percentages of cell staining. Data from three independent experiments were pooled ($n = 15$). (F) Graph showing relative RNA levels of viral M protein in the lungs of infected mice after primary infection and reinfection with 500 PFU PR/8. *, $P < 0.05$; **, $P < 0.01$ (determined using the Mann-Whitney test).

how antigen-specific CD8 T cells directly respond to IFN-γ signals during infection may provide important clues as to how the immune system regulates the survival of only a small proportion of effector CD8 T cells for memory cell generation. T-bet is a transcription factor that regulates the levels of IL-7Rα, and T-bet deficiency leads to increased levels of IL-7Rα-expressing CD8 T cells at the peak of the response (30). Inhibition of T-bet expression due to IFN-γ deficiency could lead to the increased levels of IL-7Rα on virus-specific CD8 T cells.

Our findings with IFN-$\gamma^{-/-}$ mice infected with the PR/8 or HKx31 strain of influenza virus differ from previously published data for IFN-$\gamma^{-/-}$ mice (31), wherein a defect in migration of the antigen-specific CD8 T cells to the lung and concomitant accumulation in the spleen were reported. However, our results are consistent with previous observations in terms of lung viral load and resolution (no difference seen in the absence of IFN-γ signaling), an aspect controlled by the CD8 T cell response in the lung. Furthermore, it is important to note that evaluation of the BAL fluid

does not provide a comprehensive evaluation of the CD8 T cell response in the lung and could be attributed to the possible differences observed between the studies. Although several recent studies show that IFN-γ may influence the trafficking and contraction of the CD8 T cell response against LCMV and *Listeria* infections (18, 19), others have reported that IFN-γ does not play a role in the contraction of CD8 T cell responses after CMV and VSV infections (20, 21). This suggests that the effects of IFN-γ on the magnitude of CD8 T cell contraction may be specific to the particular pathogen. A likely explanation is that the inflammatory cytokine milieu induced by the pathogen may balance the effect of IFN-γ signaling on the CD8 T cells to influence their survival and contraction. Consistent with this hypothesis, it was observed that airway epithelial cells produce IL-15 following influenza virus infection (32), and infection with LCMV induces an expansion in IL-7-producing stromal cells in the secondary lymphoid organs (33).

Current vaccination strategies have failed to elicit a strong and lasting CD8 T cell response against influenza virus that provides heterosubtypic immunity. Some studies have shown that limiting the inflammation phase during infection can reduce the contraction phase, thereby increasing the number of memory precursors, and also keeping tissue damage in check (11). Our results suggest that modulation of IFN-γ levels to increase IL-7Rα expression on effector CD8 T cells represents a potential strategy to increase the numbers of CD8 T cell memory precursors, thus permitting the development of an effective memory response to influenza virus. Our studies provide strong evidence supporting a T cell-intrinsic role for IFN-γ in limiting the magnitude of the memory CD8 T cell pool against influenza virus. These findings advance our understanding of CD8 T cell homeostasis and have implications for the development of more effective vaccines against influenza.

ACKNOWLEDGMENTS

REFERENCES

1. Hensley SE, Das SR, Bailey AL, Schmidt LM, Hickman HD, Jayaraman A, Viswanathan K, Raman R, Sasisekharan R, Bennink JR, Yewdell JW. 2009. Hemagglutinin receptor binding avidity drives influenza A virus antigenic drift. Science 326:734–736.
2. Townsend AR, Skehel JJ. 1982. Influenza A specific cytotoxic T-cell clones that do not recognize viral glycoproteins. Nature 300:655–657.
3. Townsend AR, Skehel JJ, Taylor PM, Palese P. 1984. Recognition of influenza A virus nucleoprotein by an H-2-restricted cytotoxic T-cell clone. Virology 133:456–459.
4. McMichael AJ, Gotch FM, Noble GR, Beare PA. 1983. Cytotoxic T-cell immunity to influenza. N. Engl. J. Med. 309:13–17.
5. Topham DJ, Tripp RA, Doherty PC. 1997. CD8+ T cells clear influenza virus by perforin or Fas-dependent processes. J. Immunol. 159:5197–5200.
6. Yap KL, Ada GL, McKenzie IF. 1978. Transfer of specific cytotoxic T lymphocytes protects mice inoculated with influenza virus. Nature 273:238–239.
7. Ho AW, Prabhu N, Betts RJ, Ge MQ, Dai X, Hutchinson PE, Lew FC, Wong KL, Hanson BJ, Macary PA, Kemeny DM. 2011. Lung CD103+

8. Lawrence CW, Ream RM, Braciale TJ. 2005. Frequency, specificity, and sites of expansion of CD8+ T cells during primary pulmonary influenza virus infection. J. Immunol. 174:5332–5340.
9. GeurtsvanKessel CH, Willart MA, van Rijt LS, Muskens F, Kool M, Baas C, Thielemans K, Bennett C, Clausen BE, Hoogsteden HC, Osterhaus AD, Rimmelzwaan GF, Lambrecht BN. 2008. Clearance of influenza virus from the lung depends on migratory langerin+CD11b− but not plasmacytoid dendritic cells. J. Exp. Med. 205:1621–1634.
10. La Gruta NL, Rothwell WT, Cukalac T, Swan NG, Valkenburg SA, Kedzierska K, Thomas PG, Doherty PC, Turner SJ. 2010. Primary CTL response magnitude in mice is determined by the extent of naive T cell recruitment and subsequent clonal expansion. J. Clin. Invest. 120:1885–1894.
11. Badovinac VP, Porter BB, Harty JT. 2004. CD8+ T cell contraction is controlled by early inflammation. Nat. Immunol. 5:809–817.
12. Joshi NS, Cui W, Chandele A, Lee HK, Urso DR, Hagman J, Gapin L, Kaech SM. 2007. Inflammation directs memory precursor and short-lived effector CD8(+) T cell fates via the graded expression of T-bet transcription factor. Immunity 27:281–295.
13. Williams MA, Bevan MJ. 2007. Effector and memory CTL differentiation. Annu. Rev. Immunol. 25:171–192.
14. Pipkin ME, Sacks JA, Cruz-Guilloty F, Lichtenheld MG, Bevan MJ, Rao A. 2010. Interleukin-2 and inflammation induce distinct transcriptional programs that promote the differentiation of effector cytolytic T cells. Immunity 32:79–90.
15. Kalia V, Sarkar S, Subramaniam S, Haining WN, Smith KA, Ahmed R. 2010. Prolonged interleukin-2Ralpha expression on virus-specific CD8+ T cells favors terminal-effector differentiation in vivo. Immunity 32:91–103.
16. Schluns KS, Kieper WC, Jameson SC, Lefrancois L. 2000. Interleukin-7 mediates the homeostasis of naive and memory CD8 T cells in vivo. Nat. Immunol. 1:426–432.
17. Becker TC, Wherry EJ, Boone D, Murali-Krishna K, Antia R, Ma A, Ahmed R. 2002. Interleukin 15 is required for proliferative renewal of virus-specific memory CD8 T cells. J. Exp. Med. 195:1541–1548.
18. Badovinac VP, Tvinnereim AR, Harty JT. 2000. Regulation of antigen-specific CD8+ T cell homeostasis by perforin and interferon-gamma. Science 290:1354–1358.
19. Tewari K, Nakayama Y, Suresh M. 2007. Role of direct effects of IFN-gamma on T cells in the regulation of CD8 T cell homeostasis. J. Immunol. 179:2115–2125.
20. Andrews DM, Andoniou CE, Fleming P, Smyth MJ, Degli-Esposti MA. 2008. The early kinetics of cytomegalovirus-specific CD8+ T-cell responses are not affected by antigen load or the absence of perforin or gamma interferon. J. Virol. 82:4931–4937.
21. Christensen JE, Wodarz D, Christensen JP, Thomsen AR. 2004. Perforin and IFN-gamma do not significantly regulate the virus-specific CD8+ T cell response in the absence of antiviral effector activity. Eur. J. Immunol. 34:1389–1394.
22. Kandasamy M, Ying PC, Ho AW, Sumatoh HR, Schlitzer A, Hughes TR, Kemeny DM, Morgan BP, Ginhoux F, Sivasankar B. 2013. Complement mediated signaling on pulmonary CD103(+) dendritic cells is critical for their migratory function in response to influenza infection. PLoS Pathog. 9:e1003115. doi:10.1371/journal.ppat.1003115.
23. Betts RJ, Prabhu N, Ho AW, Lew FC, Hutchinson PE, Rotzschke O, Macary PA, Kemeny DM. 2012. Influenza A virus infection results in a robust, antigen-responsive, and widely disseminated Foxp3+ regulatory T cell response. J. Virol. 86:2817–2825.
24. Badovinac VP, Porter BB, Harty JT. 2002. Programmed contraction of CD8(+) T cells after infection. Nat. Immunol. 3:619–626.
25. Kaech SM, Tan JT, Wherry EJ, Konieczny BT, Surh CD, Ahmed R. 2003. Selective expression of the interleukin 7 receptor identifies effector CD8 T cells that give rise to long-lived memory cells. Nat. Immunol. 4:1191–1198.
26. Refaeli Y, Van Parijs L, Alexander SI, Abbas AK. 2002. Interferon gamma is required for activation-induced death of T lymphocytes. J. Exp. Med. 196:999–1005.
27. Liu Y, Janeway CA, Jr. 1990. Interferon gamma plays a critical role in induced cell death of effector T cell: a possible third mechanism of self-tolerance. J. Exp. Med. 172:1735–1739.
28. Gajewski TF, Fitch FW. 1988. Anti-proliferative effect of IFN-gamma

in immune regulation. I. IFN-gamma inhibits the proliferation of Th2 but not Th1 murine helper T lymphocyte clones. J. Immunol. **140:** 4245–4252.

29. **Vukmanovic-Stejic M, Vyas B, Gorak-Stolinska P, Noble A, Kemeny DM.** 2000. Human Tc1 and Tc2/Tc0 CD8 T-cell clones display distinct cell surface and functional phenotypes. Blood **95:**231–240.

30. **Intlekofer AM, Takemoto N, Kao C, Banerjee A, Schambach F, Northrop JK, Shen H, Wherry EJ, Reiner SL.** 2007. Requirement for T-bet in the aberrant differentiation of unhelped memory CD8+ T cells. J. Exp. Med. **204:**2015–2021.

31. **Turner SJ, Olivas E, Gutierrez A, Diaz G, Doherty PC.** 2007. Disregulated influenza A virus-specific CD8+ T cell homeostasis in the absence of IFN-gamma signaling. J. Immunol. **178:**7616–7622.

32. **Verbist KC, Cole CJ, Field MB, Klonowski KD.** 2011. A role for IL-15 in the migration of effector CD8 T cells to the lung airways following influenza infection. J. Immunol. **186:**174–182.

33. **Onder L, Narang P, Scandella E, Chai Q, Iolyeva M, Hoorweg K, Halin C, Richie E, Kaye P, Westermann J, Cupedo T, Coles M, Ludewig B.** 2012. IL-7-producing stromal cells are critical for lymph node remodeling. Blood **120:**4675–4683.